

Perfluorocyclobutane (PFC-318, $c\text{-C}_4\text{F}_8$) in the global atmosphere

Mühle et al., acp-2019-267

Supplemental text, figures, and tables

AGAGE in situ data are available at

<http://agage.mit.edu/data>

<http://cdiac.ess-dive.lbl.gov/ndps/alegage.html>

CSIRO and Bristol inversion results, firm data, etc. are given in

Mühle et al. $c\text{-C}_4\text{F}_8$ acp-2019-267 Supplemental tables.xlsx

Details on bottom-up emission inventories (UNFCCC, EDGAR, NIRs, WSC) for $c\text{-C}_4\text{F}_8$

Amongst the countries reporting to the United Nations Framework Convention on Climate Change (UNFCCC) (2016), a few countries report $c\text{-C}_4\text{F}_8$ emissions, most notably France, the USA, and Russia, and the global total ranges from 7 (1993) to 26 (2011) t yr^{-1} ($0.007\text{--}0.026 \text{ Gg yr}^{-1}$, $1 \text{ t} = 1 \text{ metric ton} = 1 \text{ tonne} = 0.001 \text{ Gg}$). Several countries also or exclusively report emissions of an unspecified mix of PFCs as a sum of CO_2 -equivalent ($\text{CO}_2\text{-eq.}$) emissions (using global warming potentials, GWP), which may contain $c\text{-C}_4\text{F}_8$ emissions, most notably Japan (3,260 (2013) – 19,900 (1997) $\text{Gg CO}_2\text{-eq.}$), followed by much smaller amounts from France (~ 139 (2000) – 518 (2012) $\text{Gg CO}_2\text{-eq.}$) and a few other European countries.

Based on the National Inventory Report (NIR) for France, their reported emissions of unspecified mix of PFCs, all from category 2G2 (SF_6 and PFCs from other product use), does not contain any $c\text{-C}_4\text{F}_8$.

Based on the NIR for the Netherlands and Austria, category 2E1 (integrated circuit (IC) or semiconductor (SC) production) could contribute a few to a few ten t yr^{-1} of $c\text{-C}_4\text{F}_8$ per country if all emissions of unspecified mix of PFCs were $c\text{-C}_4\text{F}_8$, which is very unlikely. More likely seems that the GWP weighted mix of fugitive emissions from category 2E1 from these countries is similar to the mix for category 2E1 from European countries which report individual emissions for category 2E1. For the European Union, $c\text{-C}_4\text{F}_8$ represents $\sim 0\text{--}8\%$ of the GWP weighted PFC mix (CF_4 , C_2F_6 , C_3F_8 , $c\text{-C}_4\text{F}_8$) from 2E1. If the Netherlands and Austria emit 8% of GWP weighted mix of PFCs in category 2E1 as $c\text{-C}_4\text{F}_8$, this would sum up to at most a few t yr^{-1} .

The United Kingdom NIR details that their unspecified PFC mix emissions are all from category 2B9 (fluorochemical production) and refers to the UK environmental agency's pollution inventory (<https://data.gov.uk/dataset/pollution-inventory>). Judging from this inventory and our knowledge of the listed PFC sources, they most likely do not emit any $c\text{-C}_4\text{F}_8$ and thus category 2B9 does not contain any $c\text{-C}_4\text{F}_8$ emissions for the UK.

The Japanese NIR details that their emissions of unspecified mix of PFCs stems from categories 2B9, 2E (SC, liquid crystals, and photovoltaic production), and 2F5 (solvents use). For Japan, category 2F5 is comprised of C_3F_{14} and

36 C₆F₁₆ emissions, but no *c*-C₄F₈. *c*-C₄F₈ emissions from category 2E can be estimated using purchased amounts of *c*-
37 C₄F₈ from the NIR and IPCC emission estimation methods (IPCC, 2006) and are likely at most a few t yr⁻¹. If all of
38 Japan's emissions from category 2B9 (fugitive emissions from fluorochemical production) were *c*-C₄F₈, this could
39 equate to several tens to two hundred t yr⁻¹. However, more likely is that the PFC emissions from category 2B9 are
40 due to fugitive emissions from PFC production in Japan, and that their mix is similar to the PFC mix used in Japan
41 for the electronics industries (2E) of CF₄, C₂F₆, C₃F₈, and *c*-C₄F₈. As detailed in the NIR, *c*-C₄F₈ used in category 2E
42 represents 0–7 % of the total PFC mix (CO₂-eq.), which would equate to a few t yr⁻¹ from category 2B9. The
43 Netherlands also lists unspecified PFC mix emissions from category 2B9. If we assume a similar mix as for Japan,
44 this would contribute less than 0.6 t yr⁻¹ of *c*-C₄F₈.

45 Two countries report emissions of an unspecified mix of HFCs and PFCs and other fluorinated compounds to the
46 UNFCCC, the United States of America (293 (1990) – 9449 (2014) Gg CO₂-eq.) and Germany (152 (2014) – 5773
47 (1995) Gg CO₂-eq.). The German NIR details that their emissions of unspecified mix of PFCs and HFCs and other
48 fluorinated compounds is comprised of various HFCs, hydrofluoroethers (HFE), C₃F₈, higher PFCs, perfluorinated
49 polyether (PFPE), anesthetics, and SF₆ from categories 2B9 and 2H3 (Others), but not *c*-C₄F₈.

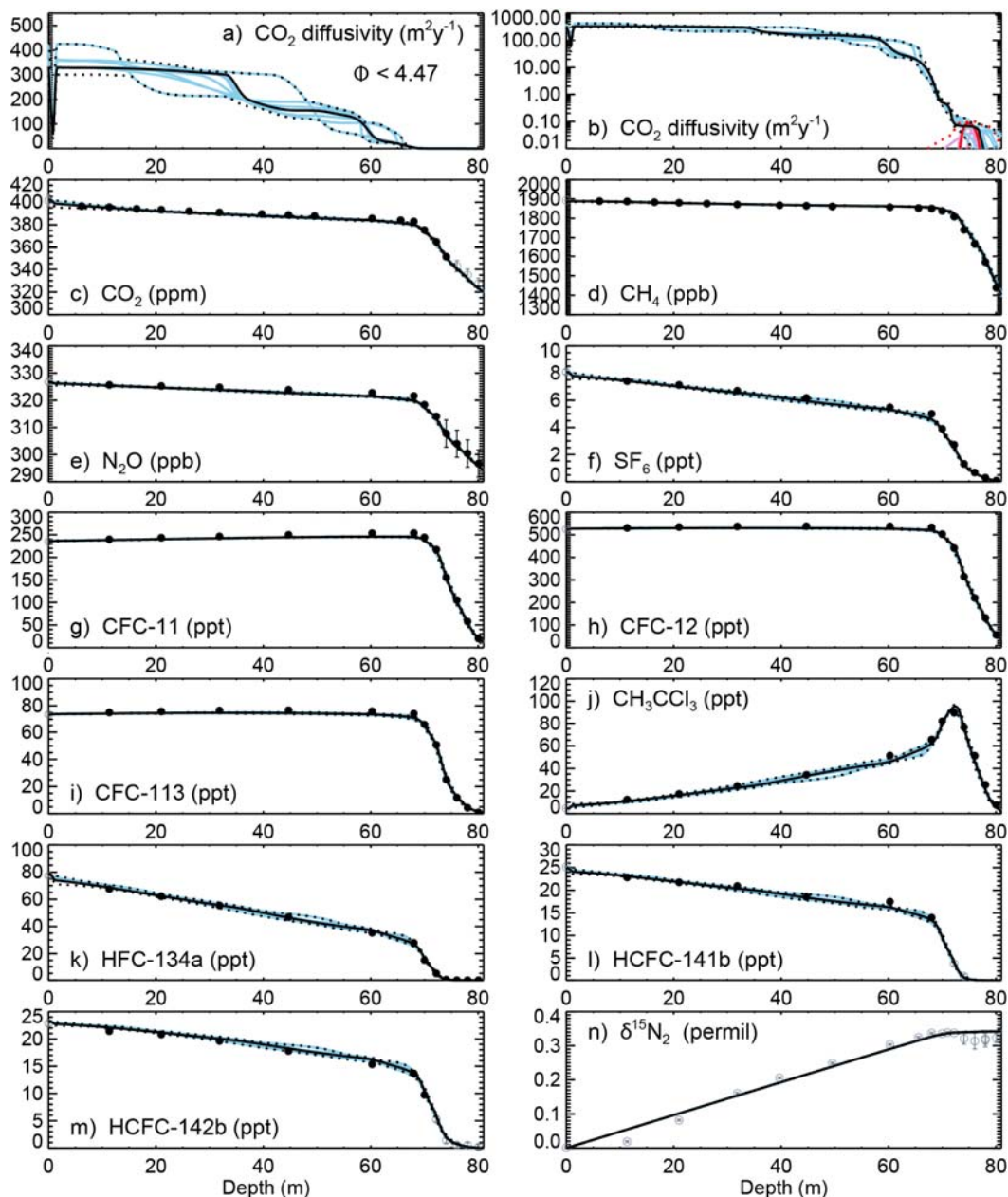
50 The US reports *c*-C₄F₈ emissions of a few t yr⁻¹ from category 2E1 (IC or SC production). The NIR details that the
51 US emissions of unspecified mix of PFCs and HFCs and other fluorinated compounds stems from category 2F6
52 (product uses as substitutes of ozone depleting substances (ODSs), other applications). From the description of
53 category 2F and subcategory 2F6 it seems likely that *c*-C₄F₈ is at most a minor component of category 2F6 which is
54 comprised of various HFCs, HFOs, C₄F₁₀, and a diverse collection of PFCs and PFPEs employed for solvent
55 applications. Based on this one may conclude that no additional *c*-C₄F₈ emissions occur. However, data from the US
56 EPA (https://www.epa.gov/sites/production/files/2018-10/ghgrp_i_freq_request_data_8_19_2018.xlsx, accessed Jan
57 2019) details that *c*-C₄F₈ emissions from three fluorochemical production facilities in the eastern US ranged from 29
58 to 62 t yr⁻¹ from 2011 to 2017. At least two of these facilities are known to produce TFE, HFP, and/or PTFE and it is
59 likely that these facilities use the process via pyrolysis of HCFC-22, with *c*-C₄F₈ as an intermediate/by-product,
60 which probably is the source of these reported emissions. These *c*-C₄F₈ emissions, which are ~8 times larger than the
61 emissions listed *c*-C₄F₈ emissions from category 2E, are currently not reported in category 2B9 (fluorochemical
62 production). The US EPA intends to report these emissions once emissions for the years 1990 to 2010 have been
63 estimated (currently only data from 2011 onward exists) to fulfil UNFCCC reporting requirements to estimate
64 emissions for each year since 1990 (US EPA, personal communication). It is unclear if these *c*-C₄F₈ emissions are
65 currently reported in the unspecified mix of PFCs and HFCs and other fluorinated compounds.

66 In summary, data submitted to UNFCCC probably represent 10–30 t yr⁻¹ (0.01–0.03 Gg yr⁻¹) of *c*-C₄F₈ emissions,
67 with 25–30 t yr⁻¹ (0.025–0.030 Gg yr⁻¹) from 2011 to 2014. After adding the US emissions from fluorochemical
68 production listed by the US EPA, this increases substantially to 50–83 t yr⁻¹ (0.05–0.083 Gg yr⁻¹) from 2011 to 2014.
69 It seems that large uncertainties remain due to difficulties disentangling the emissions of unspecified mixes of PFCs
70 and mixes of HFCs/PFCs/other fluorinated compounds and perhaps unquantified or unaccounted for emissions.

71 The Emissions Database for Global Atmospheric Research (EDGAR) aims to estimate global emissions, including
72 from countries not reporting to the UNFCCC, most notably China, South Korea, and Taiwan which may have
73 significant *c*-C₄F₈ emissions from their electronics and PTFE industries. EDGAR v4.2 (EDGAR, 2010) estimates

74 global *c*-C₄F₈ emission from three sources (SC production, solvent use, fire extinguisher use), but only until 2010.
75 From 1970 to 1985, EDGAR reports no *c*-C₄F₈ emissions, followed by a rise to a few t yr⁻¹ in the early 1990s and to
76 ~25 t yr⁻¹ (~0.025 Gg yr⁻¹) in 2008, followed by a decline to ~20 t yr⁻¹ (0.02 Gg yr⁻¹) in 2010.
77 For Japan, *c*-C₄F₈ emissions reported by EDGAR are broadly consistent with those calculated from the UNFCCC
78 NIR (see above) from the electronics industry alone (category 2E, assuming an increasing fraction of abatement from
79 2005 forward); therefore the potential emissions from category 2B9 (fugitive emissions from fluorochemical
80 production) estimated above do not seem to be included in EDGAR.
81 For South Korea a NIR with data until 2013 can also be obtained (<http://www.gir.go.kr/eng/>). EDGAR *c*-C₄F₈
82 emission estimates are broadly consistent with those estimated from the South Korean NIR using IPCC
83 methodologies for the electronics industries (category 2E), a few t yr⁻¹ until 2010.
84 For Taiwan we received *c*-C₄F₈ emissions from their NIR (Chang-Feng Ou-Yang, personal communications).
85 Emissions reported by EDGAR are consistently lower than given in the NIR, at most a t yr⁻¹ versus a few t yr⁻¹ (since
86 2001) to ~20 t yr⁻¹ (2014). The Taiwanese NIR only includes emissions from SC, IC, and memory production,
87 potentially excluding other emission sources, such as from LCD/TFT production. For China, Malaysia, and
88 Singapore, EDGAR lists only very small emissions of less than a t yr⁻¹. Particularly for China this seems unlikely due
89 to its large electronics and PTFE industries, potential *c*-C₄F₈ sources.
90 The World Semiconductor Council (WSC) estimates PFC emissions from their member industries in China, Taiwan,
91 Europe, Japan, South Korea, United States, which range from 14 t yr⁻¹ in 2012 to 24 t yr⁻¹ in 2016.
92 Based on the available information discussed above we constructed a bottom-up inventory. First, we added for each
93 year and each country emissions reported to UNFCCC and the estimated portion from unspecified mix of PFCs. For
94 2011 to 2014 we also added the U.S. emissions from fluorocarbon production reported by US EPA. Then we
95 calculated the maximum for each year and each country from these augmented UNFCCC data, US EPA, EDGAR,
96 and estimates from the NIRs, as detailed above. Globally these add up to 10–30 t yr⁻¹ (0.01–0.03 Gg yr⁻¹) from 1990
97 to 1999, 30–40 t yr⁻¹ (0.03–0.04 Gg yr⁻¹) from 2000 to 2010, and 100–116 t yr⁻¹ (~0.1 Gg yr⁻¹) from 2011 to 2014
98 (with a substantial fraction due to the U.S. emissions from fluorocarbon production reported by US EPA). WSC
99 emissions discussed above corresponds to ~16 % of these global emissions for the years 2012 to 2014.

100
101
102
103
104
105
106
107
108
109
110
111



113
 114 **Figure S1.** Tuning of the CSIRO firm model for the Summit13 site: CO₂ diffusivity on linear and log scales, and
 115 concentration profiles of CO₂, CH₄, N₂O, SF₆, CFC-11, CFC-12, CFC-113, CH₃CCl₃, HFC-134a, HCFC-141b, and
 116 HCFC-142b, as well as the δ¹⁵N₂ profile. The solid black lines show the case with the closest match to all
 117 observations used for diffusivity calibration. The dotted black lines show the upper and lower ranges of all cases that
 118 correspond approximately to a 68 % confidence interval. The blue curves show some representative cases within the
 119 68 % confidence interval that are used in the CSIRO inversion to incorporate firm model uncertainty. In a) and b), the
 120 black and blue lines show molecular diffusivity, while in b), the red lines show dispersion in the lock-in zone (the red
 121 solid line is our best case, red dotted lines correspond to the 68 % confidence interval, and the pink lines show some
 122 representative cases). Measurements shown by black circles were used for calibration, and measurements shown by
 123 the grey circles were not used (see text).

124 We use firm air data for 11 tracers from the Summit13, Greenland site (CO_2 , CH_4 , N_2O , SF_6 , CFC-11, CFC-12, CFC-
125 113, CH_3CCl_3 , HFC-134a, HCFC-141b, and HCFC-142b), to calibrate the diffusivity-depth profile and other
126 diffusivity-related parameters in the CSIRO firm model using established methods. The firm model includes
127 molecular diffusion throughout the firm (Schwander et al., 1993), and dispersion in the lock-in zone (Buizert and
128 Severinghaus, 2016). The model gives the best match to observations with dispersion in the lock-in zone peaking at
129 around $0.1 \text{ m}^2 \text{ yr}^{-1}$, consistent with Buizert et al. (2013) and Buizert and Severinghaus (2016), although there were
130 also cases within the 68 % confidence interval that had no lock-in zone dispersion. We tested the use of eddy
131 diffusion for convective mixing near the surface, but the best fit to observations was obtained without it, so it was
132 not used in the final calibration. A melt layer was observed at Summit, due to melting that occurred in July 2012.
133 The melt layer corresponds to a depth of around 60 cm but there were extensive percolated melt features down to
134 around 1.5 m. The melt layer was included in the CSIRO firm model as described in Trudinger et al. (2013). Model
135 layers in the CSIRO firm model move with the ice, and the timing of model layer generation at the surface was
136 chosen so that the influence of the melt layer began in July 2012, and extended down to a model layer boundary that
137 reached around 1.4 m at the time of firm sampling. The model produced the best fit to observations with reduction of
138 diffusion by the melt layer of around 90 % (this value depends on the location of the model layers with time). We
139 generated an ensemble of diffusivity parameters corresponding to a 68 % confidence interval as described in
140 Trudinger et al. (2013), to use this to incorporate firm model uncertainty into the inversion.

141 Figure S1 shows the optimized diffusivity-depth profile and the modelled depth profiles for the calibration tracers.
142 The atmospheric histories used to force the firm model were those compiled in Buizert et al. (2012) (based on
143 Martinerie et al., 2009) for most tracers for calibration of firm models for the NEEM site, with extension to 2013
144 using in situ measurements from either Summit in the NOAA network (for CO_2 and CH_4) or Mace Head in the
145 AGAGE network, with correction between the calibration scales used by NOAA and AGAGE where required. For
146 N_2O , we used the NOAA record at Summit, extended prior to 1998 based on the Law Dome (SH) ice core record
147 (Rubino et al., 2019) and the reconstruction by Prokopiou et al. (2017). For HCFC-141b and HCFC-142b, we
148 compiled atmospheric histories using measurements from Mace Head from late 1994, and extrapolated back to zero
149 before this. Due to the lack of information on atmospheric histories of these HCFCs before 1994, the deepest few
150 measurements of these tracers were not used for calibration (indicated by the grey symbols in Figure S1). We used
151 larger uncertainties for N_2O measurements prior to the in situ record due to the higher uncertainty in the atmospheric
152 record. We excluded the deep CO_2 measurements from calibration, because at another NH site, NEEM, all models in
153 the firm model intercomparison by Buizert et al., 2012 significantly underestimated CO_2 in the deep firm; the reason
154 for this is not currently understood but could be due to in situ production or fractionation as discussed by Buizert et
155 al. $\delta^{15}\text{N}_2$ is shown in Figure S1 but was not used for calibration because it is very sensitive to thermal effects at
156 Summit that are not included in the firm model and not important for $c\text{-C}_4\text{F}_8$.

157

158 Buizert, C., Martinerie, P., Petrenko, V. V., Severinghaus, J. P., Trudinger, C. M., Witrant, E., Rosen, J. L., Orsi, A.
159 J., Rubino, M., Etheridge, D. M., Steele, L. P., Hogan, C., Laube, J. C., Sturges, W. T., Levchenko, V. A., Smith, A.
160 M., Levin, I., Conway, T. J., Dlugokencky, E. J., Lang, P. M., Kawamura, K., Jenk, T. M., White, J. W. C., Sowers,

161 T., Schwander, J., and Blunier, T.: Gas transport in firn: multiple-tracer characterisation and model intercomparison
162 for NEEM, Northern Greenland, *Atmos. Chem. Phys.*, 12, 9, 4259-4277, 10.5194/acp-12-4259-2012, 2012.

163 Buizert, C., Sowers, T., and Blunier, T.: Assessment of diffusive isotopic fractionation in polar firn, and application
164 to ice core trace gas records, *Earth Planet. Sci. Lett.*, 361, 110-119, 10.1016/j.epsl.2012.11.039, 2013.

165 Buizert, C., and Severinghaus, J. P.: Dispersion in deep polar firn driven by synoptic-scale surface pressure
166 variability, *The Cryosphere*, 10, 5, 2099-2111, 10.5194/tc-10-2099-2016, 2016.

167 Martinerie, P., Nourtier-Mazauric, E., Barnola, J.-M., Sturges, W. T., Worton, D. R., Atlas, E., Gohar, L. K., Shine,
168 K. P., and Brasseur, G. P.: Long-lived halocarbon trends and budgets from atmospheric chemistry modelling
169 constrained with measurements in polar firn, *Atmos. Chem. Phys.*, 9, 12, 3911-3934, DOI 10.5194/acp-9-3911-2009,
170 2009.

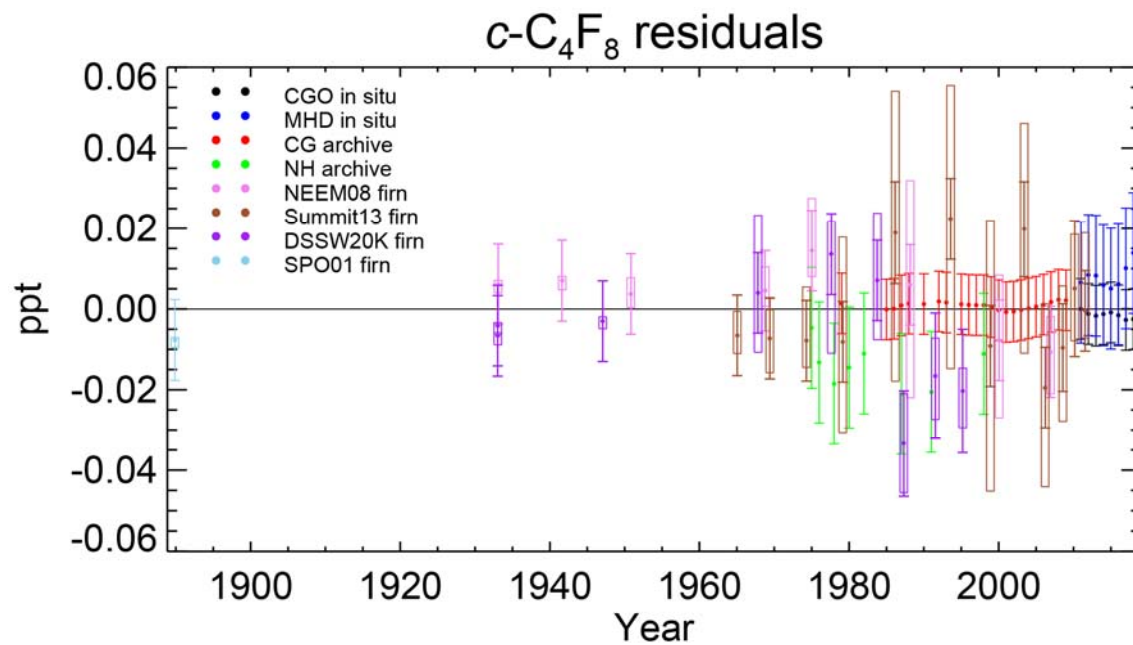
171 Prokopiou, M., Martinerie, P., Sapart, C. J., Witrant, E., Monteil, G., Ishijima, K., Bernard, S., Kaiser, J., Levin, I.,
172 Blunier, T., Etheridge, D., Dlugokencky, E., van de Wal, R. S. W., and Röckmann, T.: Constraining N₂O emissions
173 since 1940 using firn air isotope measurements in both hemispheres, *Atmos. Chem. Phys.*, 17, 7, 4539-4564,
174 10.5194/acp-17-4539-2017, 2017.

175 Rubino, M., Etheridge, D. M., Thornton, D. P., Howden, R., Allison, C. E., Francey, R. J., Langenfelds, R. L.,
176 Steele, P. L., Trudinger, C. M., Spencer, D. A., Curran, M. A. J., Van Ommen, T. D., and Smith, A. M.: Revised
177 records of atmospheric trace gases CO₂, CH₄, N₂O and $\delta^{13}\text{C}$ over the last 2000 years from Law Dome, Antarctica,
178 *Earth Syst. Sci. Data Discuss.*, 2018, 1-30, 10.5194/essd-2018-146, 2018.

179 Schwander, J., Barnola, J. M., Andrie, C., Leuenberger, M., Ludin, A., Raynaud, D., and Stauffer, B.: The Age of the
180 Air in the Firn and the Ice at Summit, Greenland, *J. Geophys. Res.*, 98, D2, 2831-2838, 1993.

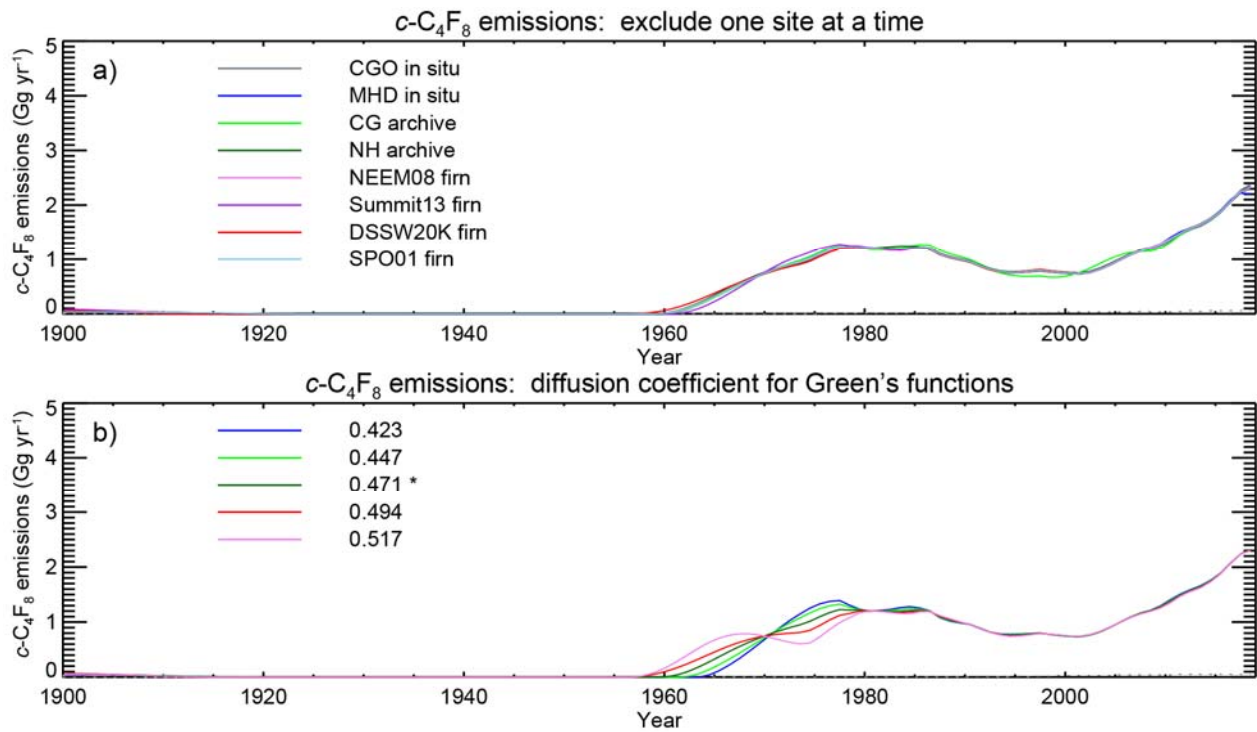
181 Trudinger, C. M., Enting, I. G., Rayner, P. J., Etheridge, D. M., Buizert, C., Rubino, M., Krummel, P. B., and
182 Blunier, T.: How well do different tracers constrain the firn diffusivity profile?, *Atmos. Chem. Phys.*, 13, 3, 1485-
183 1510, 10.5194/acp-13-1485-2013, 2013.

184
185
186
187
188
189
190
191
192
193
194
195



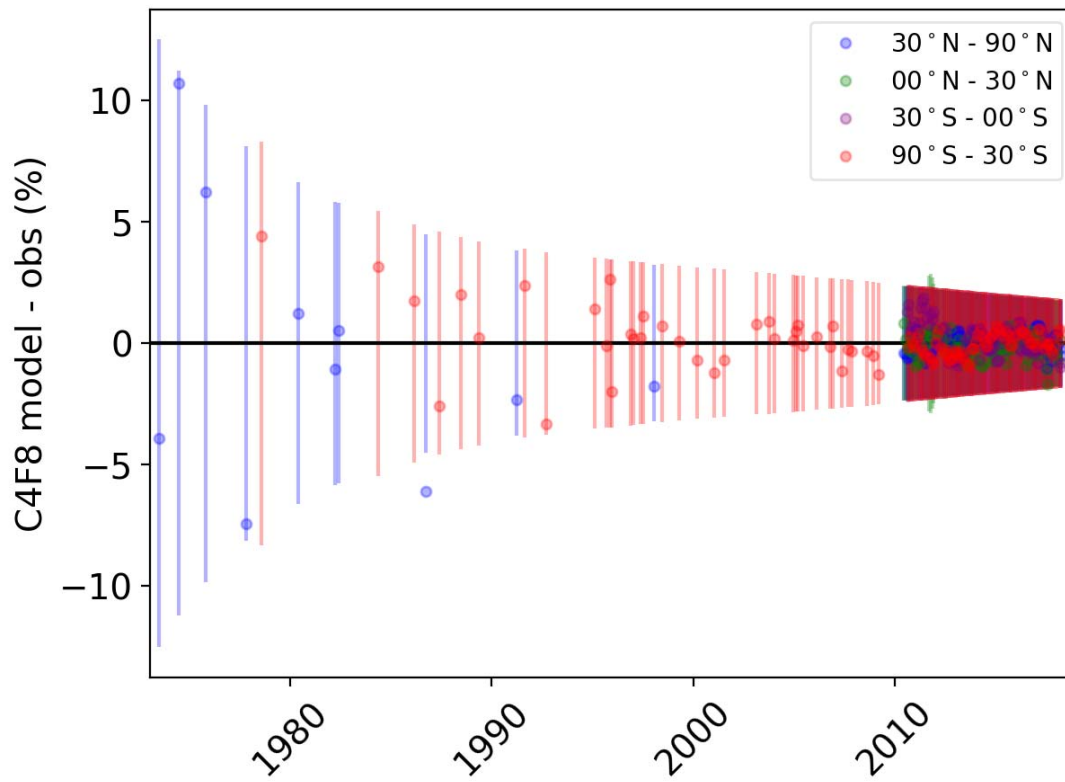
196
 197 **Figure S2.** Residuals (model - observations) for the CSIRO inversion based on firn data and annual values from the
 198 smoothing spline in each hemisphere to in situ and archive data. The error bars show measurement errors used in the
 199 inversion (for the annual values this is the magnitude of correlated errors and for the firn data these are the
 200 measurement errors with a lower threshold of 0.01 ppt). The boxes show the range of uncertainties derived from the
 201 ensemble of Green's functions from the firn model.

202
 203
 204
 205



206
 207 **Figure S3.** Sensitivity tests for the CSIRO inversion towards removal of individual data subsets and variation of the
 208 diffusion coefficient: a) inferred emissions with one firm site or in situ or archive part of the atmospheric record in
 209 each hemisphere left out at a time; b) inferred emissions for different values of the diffusion coefficient of $c\text{-C}_4\text{F}_8$
 210 relative to CO_2 , with values from -10 % to +10 %.

211
 212
 213
 214
 215
 216
 217
 218
 219
 220
 221
 222
 223
 224
 225
 226
 227



228

229 **Figure S4.** Residuals (model - observations) for the Bristol inversion based on archive and in situ data.

230

231

232

233

234

235

236

237

238

239

240

241

242

243

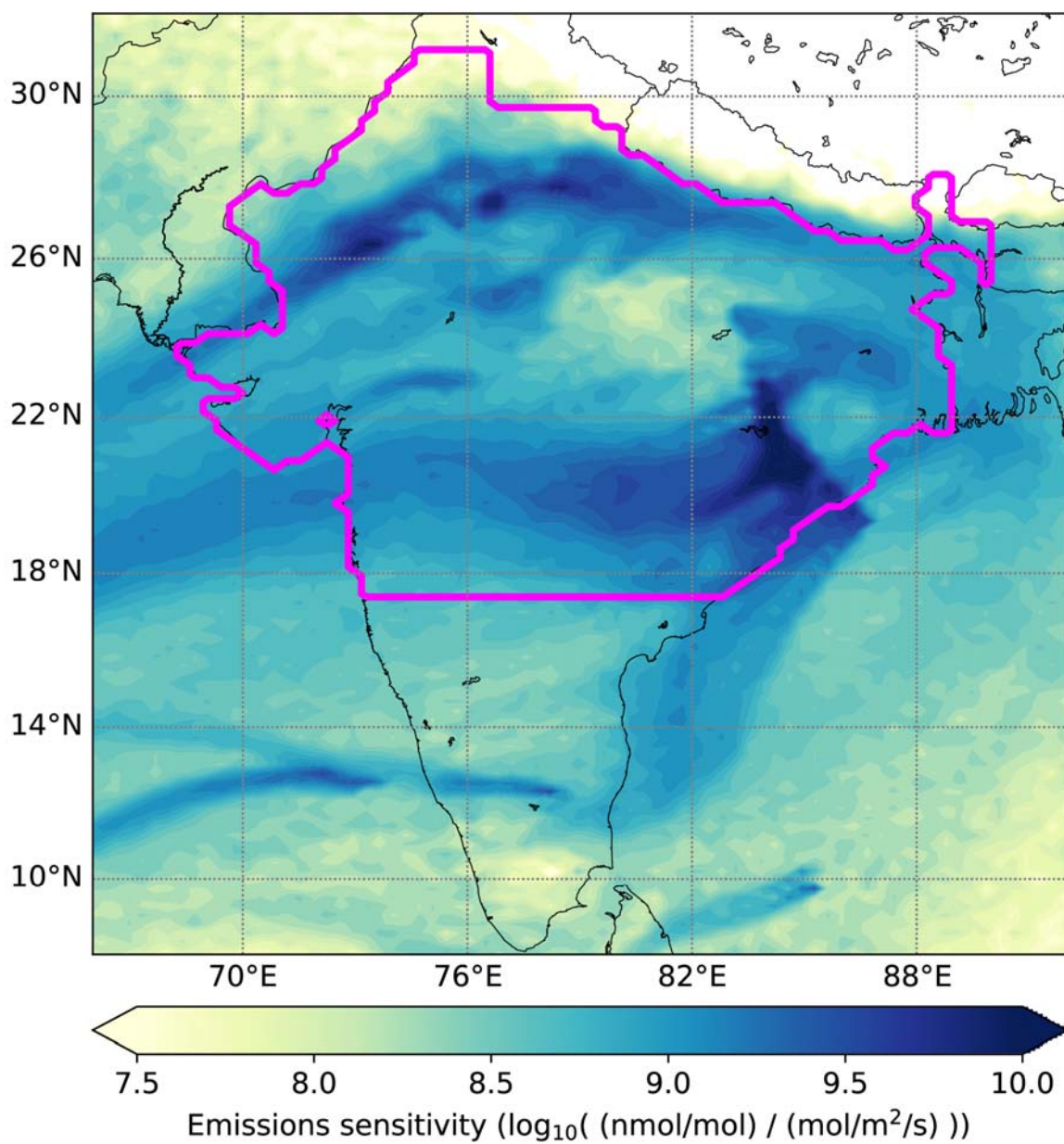
244

245

246

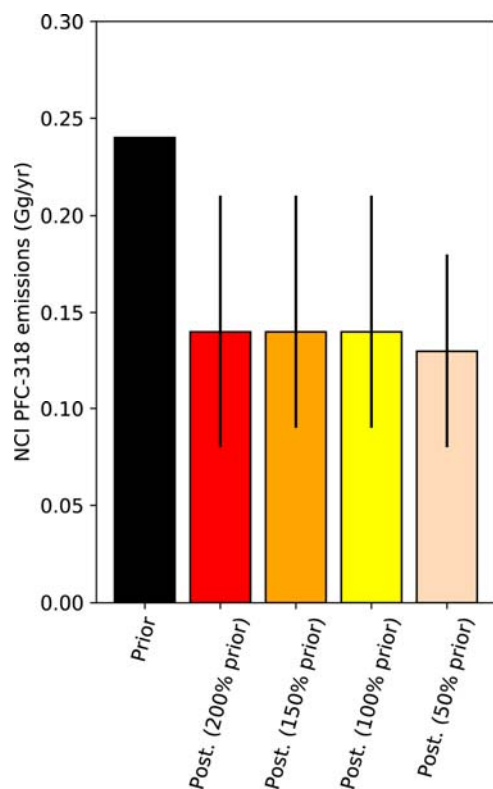
247

248



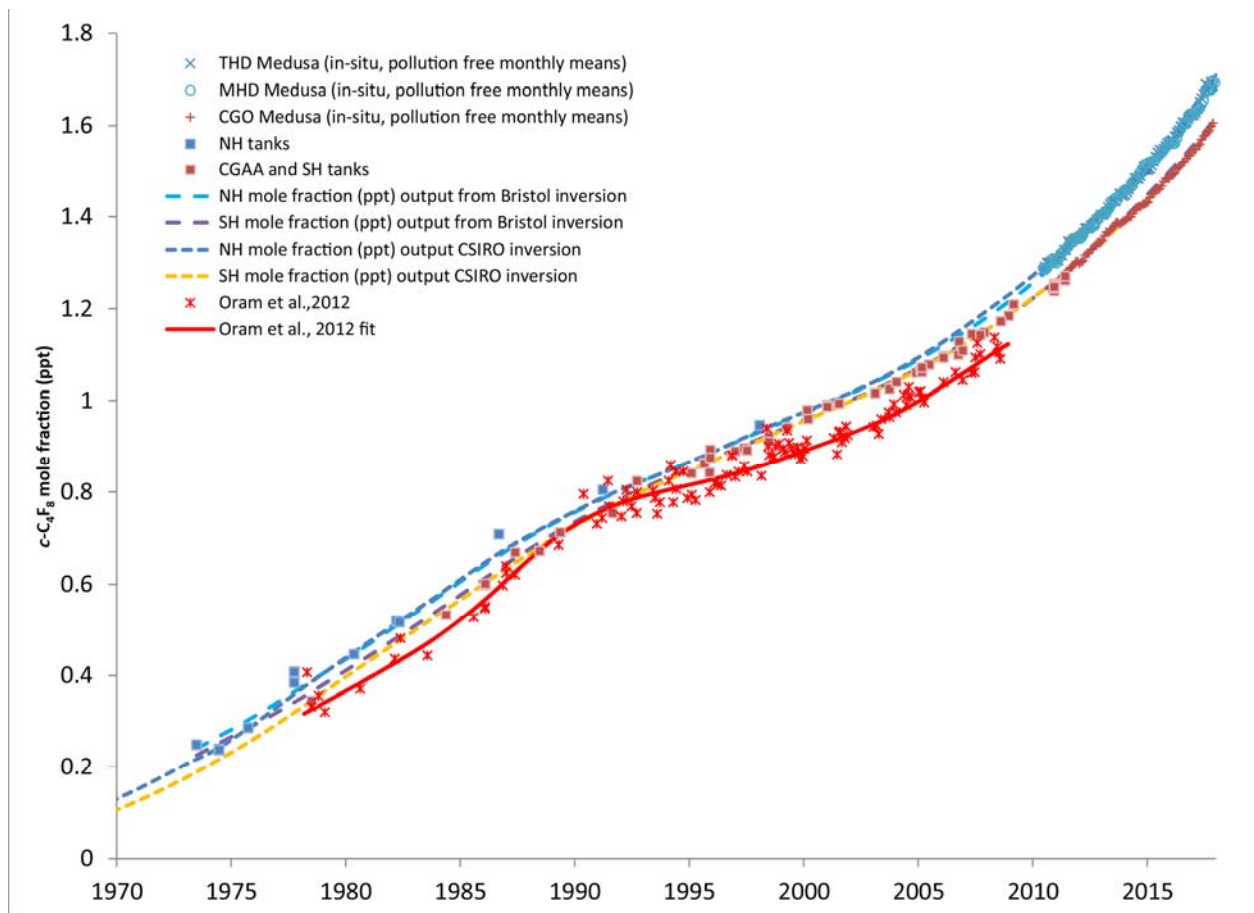
249
 250 **Figure S5:** Emissions sensitivity averaged across all measurements made over the Indian subcontinent in June and
 251 July 2016. The region roughly corresponding to a maximum in emissions sensitivity is enclosed by the pink line. We
 252 denote this region as Northern and Central India (NCI).

253
 254
 255
 256
 257
 258



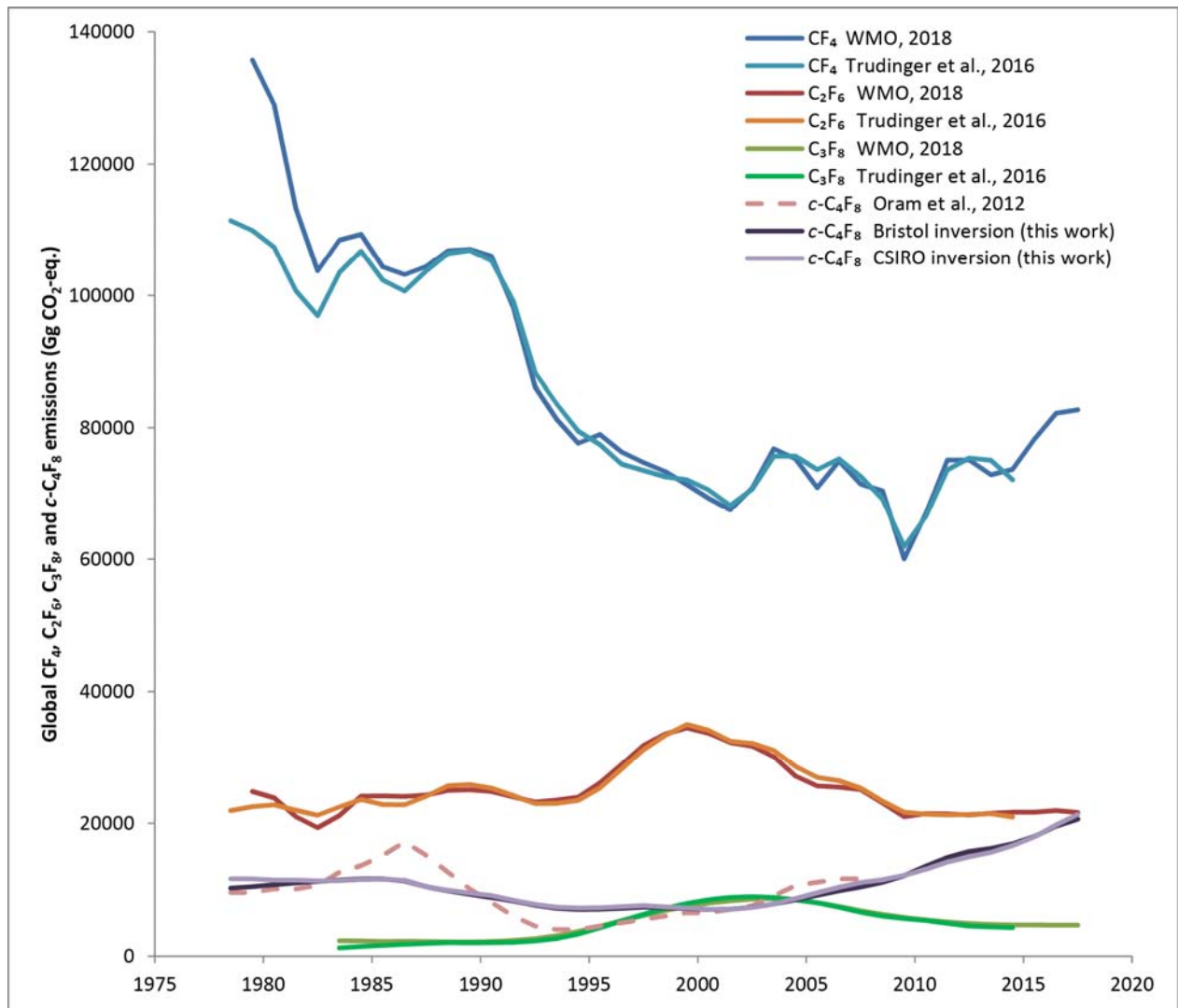
259
 260 **Figure S6:** Sensitivity tests for the NAME-HB inversion for the Indian subcontinent. Emissions derived from priors
 261 of varying magnitudes (200% of the original prior, red bar, 150% of the original prior, orange bar, and 50% of the
 262 original prior, peach bar) indicate that $c\text{-C}_4\text{F}_8$ emissions determined for Northern and Central India are very
 263 insensitive to the choice of prior. The original prior (black bar) and posterior (yellow bar) estimates are also shown.
 264 For each estimate, error bars represent the 95% confidence interval of the posterior probability density function.

265
 266
 267
 268
 269
 270
 271
 272
 273
 274
 275
 276
 277
 278
 279
 280



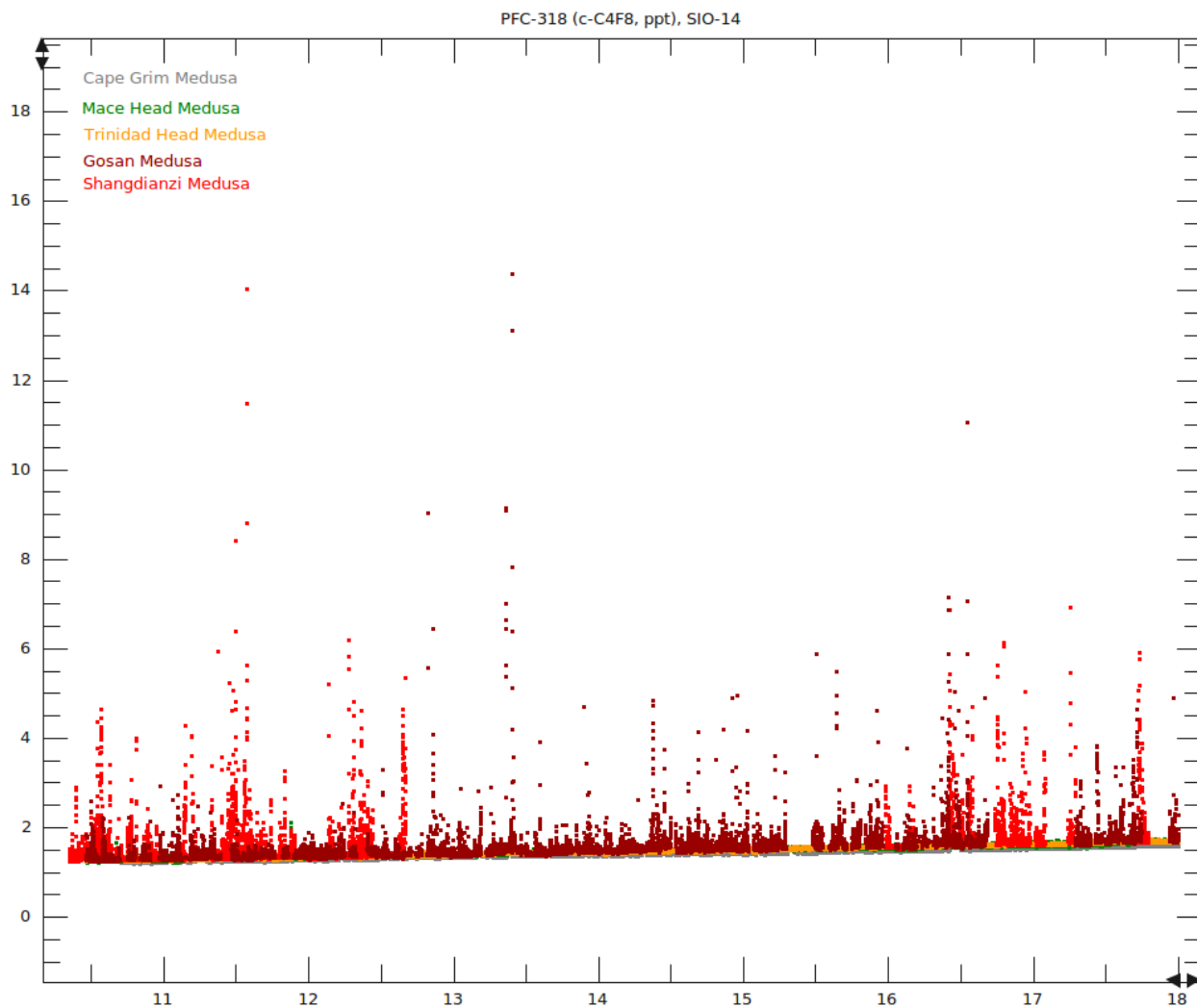
281
 282 **Figure S7.** $c\text{-C}_4\text{F}_8$ mole fractions reconstructed here for the Northern (NH) and Southern Hemisphere (SH) compared
 283 to results from Oram et al., 2012 (SH only). Measured $c\text{-C}_4\text{F}_8$ mole fractions from THD, MHD, and CGO Medusa
 284 (in situ, pollution free monthly means, blue crosses and blue circles (NH), red pluses (SH) and NH (blue squares)
 285 and CGAA and SH tanks (red squares) are shown together with results from the Bristol (AGAGE 12-box, light blue
 286 (NH) and purple (SH) long dashes) and CSIRO (dark blue (NH) and orange (SH) short dashes) inversions. $c\text{-C}_4\text{F}_8$
 287 mole fractions from Oram et al., 2012 (CGAA/SH only, red stars and red solid line) are shown for comparison.

288
 289
 290
 291
 292
 293
 294
 295
 296
 297
 298
 299



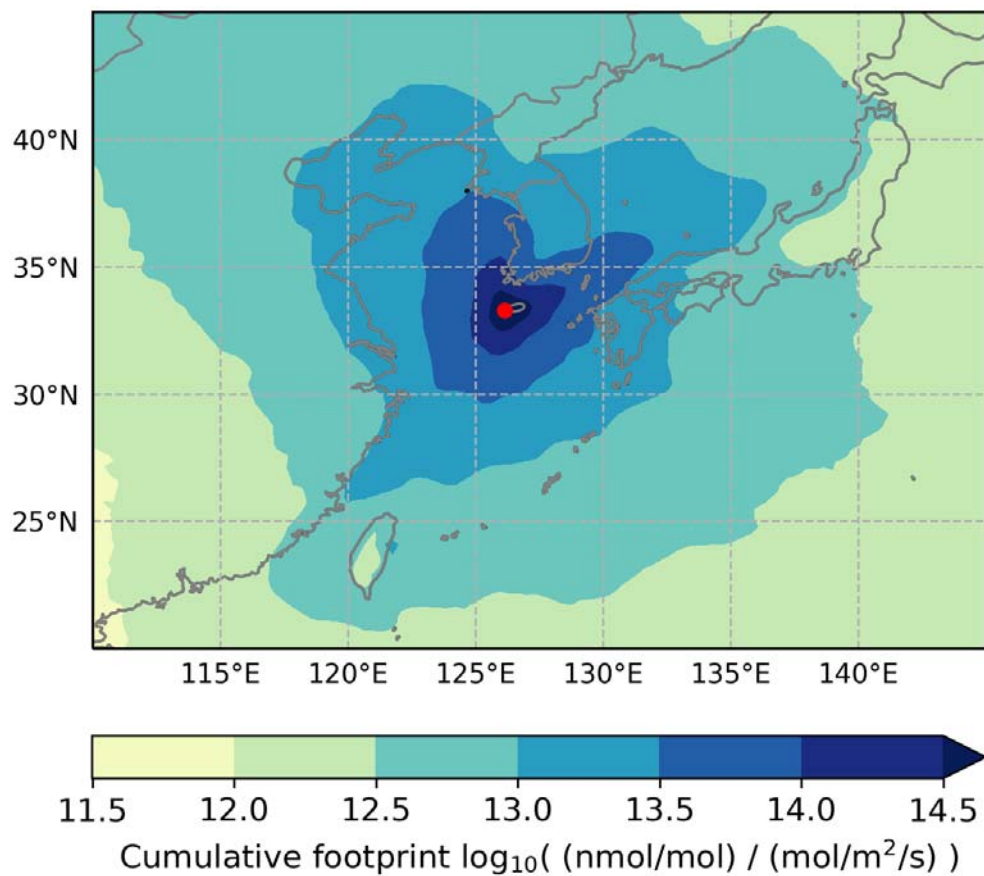
300
 301 **Figure S8:** Global emissions of CF₄, C₂F₆, C₃F₈, and c-C₄F₈ expressed as carbon dioxide equivalent emissions (CO₂-
 302 eq.) emissions (using GWP₁₀₀) (1.000.000 Gg CO₂-eq. = 1 billion tonnes CO₂-eq.). In 2017, c-C₄F₈ emissions have
 303 reached 0.021 billion tonnes of CO₂-equivalent compared to 0.083, 0.022, and 0.005 billion tonnes of CO₂-eq. for
 304 CF₄, C₂F₆, and C₃F₈.

305
 306
 307
 308
 309
 310
 311
 312

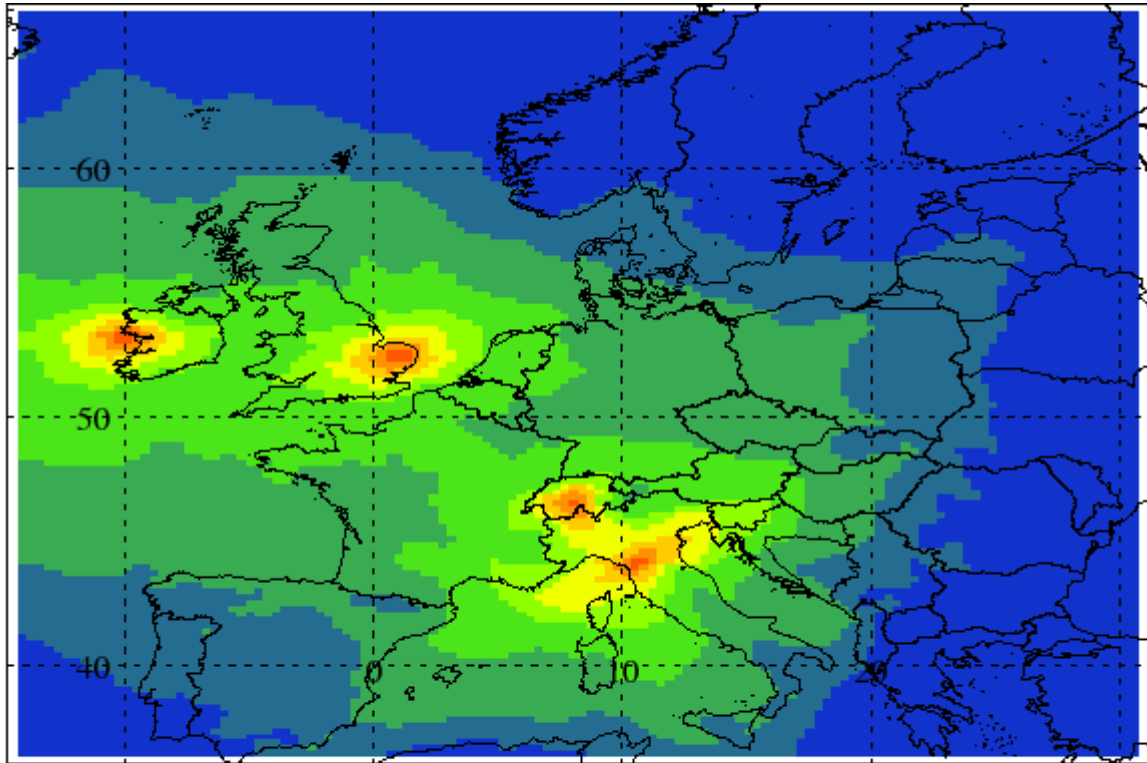


313
 314 **Figure S9.** Magnitude of pollution events in East Asia. Among all stations of the AGAGE network, the two stations
 315 in eastern Asia, Gosan (brown) and Shangdianzi (red), show by far the most frequent and most pronounced pollution
 316 events of up to ~14 ppt above NH background (Mace Head, green, Trinidad Head, orange), indicating significant
 317 regional emissions. Measurements at Cape Grim, Australia (light grey), representing SH background, are also shown
 318 for comparison.

319
 320
 321
 322
 323
 324
 325
 326
 327
 328



329
 330 **Figure S10:** Cumulative footprint map for measurements at Gosan station, Jeju island, South Korea from 2010-2017
 331 generated using the NAME transport model. The footprint indicates where the receptor station is sensitive to
 332 emissions. The sensitivity of the inversion generally decreases with distance to the receptor station resulting in
 333 relatively low sensitivity for emissions from western China, eastern Japan and Taiwan. Therefore, we report
 334 emissions for eastern China, western Japan, South Korea, North Korea, and parts of Taiwan. Eastern China contains
 335 the provinces Anhui, Beijing, Hebei, Henan, Jiangsu, Liaoning, Shandong, Shanghai, Shanxi, Tianjin and Zhejiang.
 336 Western Japan contains the prefectures Chugoku, Kansai, Shikoku and Okawa and Kyushu.
 337



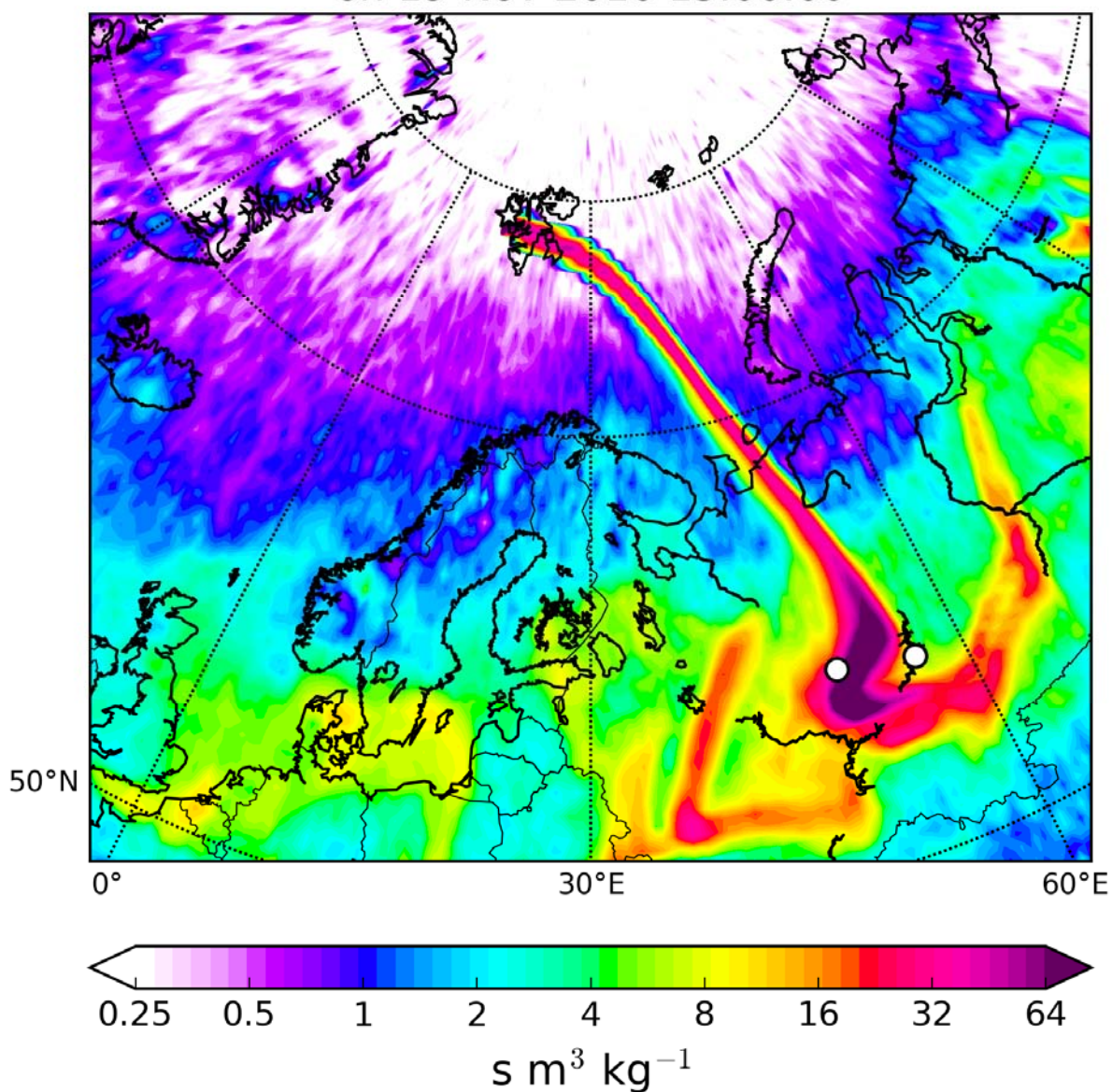
Maximum value = 4.93 g/m²/s



338 0.00 0.01 0.03 0.08 0.40
 339 **Figure S11:** Cumulative footprint map for measurements at the Tacolneston, United Kingdom, Mace Head, Ireland,
 340 Jungfrauoch, Switzerland, and Monte Cimone, Italy stations for 2013. The sensitivity of the InTEM inversion is
 341 shown in arbitrary units. We report only estimated emissions from North Western Europe (42° N to 59° N and -11° E
 342 to 15° E) based on to the areas of highest sensitivity to the observations.

343
 344
 345
 346
 347
 348
 349
 350
 351
 352
 353
 354
 355
 356

Footprint emission sensitivity
on 19-Nov-2016 15:00:00



357
358 **Figure S12.** FLEXPART backward simulation for the strong $c\text{-C}_4\text{F}_8$ pollution event observed at Zeppelin station on
359 November 19, 2016 indicate that this pollution event may be the result of direct transport of air from two facilities
360 which produce PTFE and halogenated chemicals including $c\text{-C}_4\text{F}_8$ (HaloPolymer, Kirovo-Chepetsk, Kirov Oblast
361 and Galogen Open Joint-Stock Company, Perm, Russia, each site marked with a white dot) to the Zeppelin station
362 (marked with a white star).

363
364
365
366
367

368 **Supplemental Tables**

369
 370 **Table S1.** The probability distributions assigned to the emissions and boundary conditions scaling and
 371 hyperparameters. Fixed parameters are those which have a fixed distribution that remain unchanged during the
 372 inversion. Hyperparameters represent the uncertainty in the uncertainties in the statistical model. These variable
 373 hyperparameters are estimated with their associated uncertainty within the NAME-HB inversion framework. This
 374 uncertainty translates into the total uncertainty in the posterior emissions estimates.

Parameter	Probability distribution	Fixed or variable?
Emissions and boundary conditions scaling	Log-normal(1,10)	Fixed
Model error (ppt)	Uniform(0.1, 10)	Variable
Correlation length scale (hours)	Uniform(1,120)	Variable
Number of Voronoi cells	Uniform(4,200)	Variable

375
 376 **Table S2.** Chinese production of PTFE and FEP fluoropolymers (t yr⁻¹) and five year rise rates, including 2015–2020
 377 forecast from the 13th Chinese five year plan

	2000	2005	2010	2011	2014	2015	2020*
PTFE	8,377	26,700	52,078	52,310	91,608	96,335	140,000
FEP			3,865		10,975	12,937	19,000
Fluoropolymers (total)			60,153		122,190	131,320	194,000
PTFE (% total)			87 %		75 %	73 %	72 %
FEP (% total)			6 %		9 %	10 %	10 %
% yr ⁻¹ increase		2000-2005	2005-2010			2010-2015	2015-2020*
PTFE		26 %	14 %			13 %	7.8 %
FEP						27 %	8.0 %

378 Source: www.qianzhan.com/analyst/detail/220/170629-c33a2ca7.html (Chinese, translate.google.com)

379 *Forecast from the 13th Chinese five year plan.

380
 381
 382
 383
 384
 385
 386
 387
 388
 389
 390

391 **Table S3.** Estimates of global PTFE market share by region

	2012 ⁺	2015 ⁺	2015 ⁺	2015 [#]	2015 [#]
North America	31 %	10 %		see RoW	
Europe	21 %	14 %		see RoW	
Asia Pacific (Total)	36 %	62 %		78 %	
China			53 %		67 %
Japan			9 %		11 %
Rest of World (Total)	12 %	14 %		22 %	
India			8 %		
Russia			6 %		
Total	100 %	100 %		100 %	

392 ⁺www.industry-experts.com

393 [#]www.qianzhan.com/analyst/detail/220/170629-c33a2ca7.html

394 In 2015, PTFE production in China was estimated to account for 53 - 67% of global PTFE production.

395

396 **Table S4.** Estimates of global PTFE market share by company

	2012 ⁺		2015 [#]
DuPont	31.0 %	Dupont (Global incl. China)	13 %
Daikin	14.0 %	Daikin (Global incl. China)	13 %
Solvay	11.5 %	Solvay (China)	4 %
3M	9.0 %	3M	4 %
Others	31.0 %	Shangdong Dongyue Group	20 %
		Others (China)	30 %
		Others (Global excl. China)	11 %
Arkema SA	5.5 %		
Gujarat Fluorochemicals Ltd.	3.5 %		
		Asahi Glass (Japan)	5 %
Total	100.0 %		100 %

397 ⁺www.industry-experts.com

398 [#]www.qianzhan.com/analyst/detail/220/170629-c33a2ca7.html

399 DuPont incl. Chemours, Solvay incl. Solexis, 3M incl. Dyneon, and Asahi Glass incl. AGC.

400